

Supplementary Material

Polyamine-Targeting Gefitinib Prodrug and its Near-Infrared Fluorescent Theranostic Derivative for Monitoring Drug Delivery and Lung Cancer Therapy

Xinyu Song^{1,2}, Xiaoyue Han^{2,4}, Fabiao Yu^{2,3*}, Xiaoyu Zhang^{1,2}, Lingxin Chen^{2,3*} & Changjun Lv^{1,3*}

¹ Department of Respiratory Medicine, Binzhou Medical University Hospital, Binzhou 256603, China

² Key Laboratory of Coastal Environmental Processes and Ecological Remediation, Yantai Institute of Coastal Zone Research, Chinese Academy of Sciences, Yantai 264003, China

³ Medicine Research Center, Institute of Molecular Medicine, Binzhou Medical University, Yantai 264003, China.

⁴ University of Chinese Academy of Sciences, Beijing 100049, China.

Corresponding Author: *E-mail: fbyu@yic.ac.cn; *E-mail: lxchen@yic.ac.cn; *E-mail: lucky_lcj@sina.com

Phone/fax number: +86-0535-2109130

Contents:

- 1. General Methods**
- 2. Synthesis and Characterization of Compounds**
- 3. Mechanism of PPG releasing Gefitinib**
- 4. Mechanism of TPG releasing Gefitinib and emitting NIR fluorescence**
- 5. Spectral properties and selectivity of TPG towards GSH**
- 6. Reaction kinetics of Compound 1 and GSH monitored by HPLC**
- 7. Time-dependent fluorescence intensity of TPG in PC9 cells and H1650 cells**
- 8. Images of TPG in cysteine treated PC9 cells and H1650 cells**
- 9. Images of TPG in NEM treated PC9 cells and H1650 cells**
- 10. The investigation of TPG transmembrane transport with corresponding ligand**
- 11. The investigation of TPG and TBG transmembrane transport at 4°C**
- 12. Bright-field Images of Figure 2a**
- 13. Apoptosis of H1650 cells treated with PA by flow cytometry**
- 14. Organ targeting of Probe-PA *in vivo* and *ex vivo***
- 15. Fluorescence distribution of TPG in PC9 and H1650 tumor**
- 16. Lung sections of the mice treated with the agents**
- 17. Flow cytometry analysis of TBLB samples**
- 18. Table of the patients' files**
- 19. The efficacy of Gefitinib, PA, PPG, as well as a mixture of PA and Gefitinib**
- 20. The efficacy assay of control prodrug PCG**
- 21. The prodrug stability and the release of Gefitinib assay in the presence of albumin**
- 22. The stability of *Azo*-BODIPY fluorophore**
- 23. Another format for Figure 3h and 3i**
- 24. References**

1. General Methods

Materials: The solution of Gefitinib, TPG, and PPG (1 mM) could be dissolved in dimethyl sulfoxide (DMSO) and maintained in refrigerator at 4°C, respectively. Stock solutions of cysteine (Cys), homocysteine (Hcy) and glutathione (GSH) were prepared to desired concentrations when needed. The stock solutions were diluted to desired concentrations when needed. All the reagents for chemical synthesis were purchased from Energy except 2-hydroxyethyl disulfide from Sigma-Aldrich. The reagents for spectral dynamics were purchased from Energy. HEPES (4-(2-Hydroxyethyl)-1-piperazineethanesulfonic acid) was obtained from Aladdin. The cell dyes were purchased from Thermo Fisher Scientific. CCK-8 kit was provided by Dojindo. The following rabbit monoclonal antibodies were purchased from Cell Signaling Technology (p-EGFR (Tyr1068): #3777, 1:1000; EGFR: #4267, 1:1000; p-Akt (Ser473): #4060, 1:2000; Akt: #4691, 1:1000; β -actin: #4970, 1:1000; caspase 3: #9662, 1:1000; Ki67: #12075, Alexa Fluor 647 Conjugate, 1:50) and polyclonal antibody anti-ornithine decarboxylase (#ab97395, 1:1000) were purchased from Abcam. The antibodies for flow cytometry were purchased from BD Biosciences (PE mouse anti-Akt (pS473): #560378, 20 μ L per test). EGF (recombinant human EGF, #HLM7615081) was purchased from R&D Systems. The type I collagenase were purchased from Gibco (#17018029, 200U/mL) The anti-CEA (#MA1-4809, FITC Conjugate, 1 : 25) and anti-Cytokeratin 19 (#MA5-18158, Alexa Fluor 488, 10 μ g/mL per test) were purchased from Invitrogen. Ultrapure water was used throughout.

Instruments: The ultrapure water (18.2 M Ω /cm) that was used throughout the work was obtained from a Millipore Milli-Q Ultrapure water system. Absorption spectra were examined on PerkinElmer Lambda 35 UV-visible spectrophotometer. The fluorescence spectra were detected by FluoroMax-4 Spectrofluorometer with a Xenon lamp. ¹H and ¹³C NMR spectra were acquired with a Bruker spectrometer. High-resolution mass spectra were carried on Thermo Fisher Scientific LCQ Fleet LC-MS System. The absorbances of the 96-well plate were read with a TECAN infinite M200pro microplate reader. HPLC was processed with Agilent Technologies 1260 Infinity II, equipped with a UV detector. The fluorescence images of cells were acquired using Olympus FV1000 confocal laser-scanning microscope with an objective lens (\times 20/40/60). Flow cytometry data of apoptosis and phosphorylation were collected by BD Biosciences FACSaria and data from clinical samples were collected by BD Biosciences AccuriC6. Ultrathin sections were cut using Leica EM UC7. Transmission electron microscope images were acquired with JEOL JEM-1400 transmission electron microscope. BALB/c mice and nude mice fluorescence and x-ray images were collected by Bruker *In-vivo* Imaging System. PC9 and H1650 tumor-bearing mice lung and tumor pathological sections were imaged by Nikon Model Eclipse Ci-L Microscope.

Absorption and fluorescence analysis: Absorption spectra were obtained with 1.0-cm glass cells. Fluorescence emission spectra were obtained with a Xenon lamp and 1.0-cm quartz cuvettes. The fluorescence intensity were measured at $\lambda_{ex/em} = 706/690-800$ nm for TPG and at $\lambda_{ex/em} = 704/670-800$ nm for TBG, respectively. The TPG or TBG (0.10 mL, 1.0 mM) was added to a 10.0-mL color comparison tube. After dilution to 10 μ M with 10 mM HEPES buffers, analytes were added. The mixtures were shaken for 24 h before measurement.

Cell culture: NCI-H1650 and IMR-90 cell lines were purchased from the Committee on Type Culture Collection of Chinese Academy of Sciences (Shanghai, China). PC9 cell line was purchased from European Collection of Authenticated Cell Cultures. Human non-small cell lung cancer cell lines, PC9 cells and NCI-H1650 cells, were cultured in high glucose DMEM (dulbecco's modified eagle medium) (Hyclone, USA) and RPMI (Roswell Park Memorial Institute)-1640 medium (Gibco, USA), respectively, supplemented with 10% (v/v) fetal bovine serum (Gibco, Australia) and 100 units/mL penicillin and streptomycin. Human diploid fibroblast-like cell line, IMR-90 cell line, was cultured in the complete medium comprised of MEM medium (minimum essential medium) (Gibco, USA) 87 mL, FBS 10 mL, Gluta-max (Gibco, USA) 1 mL, NEAA (Gibco, USA) 1 mL and sodium pyruvate (Gibco, USA). All cells were maintained at 37°C in a humidified atmosphere with 5% CO₂. All cells tested negative for mycoplasma with a PCR-based detection method.

CCK-8 assays: For cell survival assays, 6×10^3 cells were plated in a 96 well-plate per well. After planting cells for 24 h, the complete medium was replaced by basal medium containing 0.5% fetal calf serum. Subsequently, various concentrations of Gefitinib, TPG, and PPG were added. Then the cells were incubated for different times. The cells without any drugs were used as control. Next, the previous medium was discarded respectively and 100 μ L media containing 10% CCK-8 kit (Dojindo, Japan) (v/v) were added to each well. The plate was placed at 37°C for 1.5 h. The absorbances of the 96 well-plate at 450 nm were read using a microplate reader. The same procedure was applicable to the cells treated with PA.

Western blot analysis: All the cell samples were treated by different compounds and washed for three times before lysis of cells. Protein extracts were prepared by suspending the cells in 200 μ L RIPA lysis buffer containing 1% PMSF (Solarbio, China) and 20% PhosSTOP (Roche, Germany). Then the extracts were quantified with BCA protein assay kit (Biogot, China). After denatured, the equal amounts of protein were electrophoresed on 6–12% SDS-polyacrylamide gels (Bio-Rad, USA) and transferred to PVDF membranes. The membrane was incubated with 5% BSA (Sigma-Aldrich, USA) and incubated with primary antibodies overnight at 4°C with gentle shake. A horseradish peroxidase (HRP)-conjugated secondary antibody (Cell Signaling Technology, USA) was used to mirror the quantity of proteins and signals were detected with an enhanced chemiluminescence (ECL) detection system. The results were analyzed by ImageJ to acquire the grey value of every bond.

Transmission electron microscope imaging: After treated with PA, the cell samples were fixed in the fresh 2.5% glutaraldehyde for 5 h at 4°C and post-fixed in 1% osmium tetroxide for 1.5 h. Then the samples were dehydrated in a gradient ethanol series and infiltrated with Epon812. The samples were embedded and cured at 37°C for 12 h, 45°C for 12 h and 60°C for 24 h. Ultrathin sections were cut using Leica EM UC7 and uranyl acetate and lead citrate were used to stain the section before the observation.

Cell imaging: Fluorescent images were acquired with confocal laser scanning microscope with an objective lens ($\times 40/60$). The excitation wavelengths and emission wavelengths, which were fit in different dyes, were described in paper. PC9 and H1650 cells were planted on Petri-dishes ($\Phi = 20$ mm) and allowed to adhere for 24 h before the treatments. The prodrugs and commercial dyes were added to the culture plates which were filled with 1 mL fresh complete medium.

Flow cytometry analysis: PC9 cells and H1650 cells were plated into 2.0×10^5 cells/well in 6-well plates. After incubating the cells at 37°C with 5% CO₂ for 1–2 days to reach 80% confluency, the medium was added the compounds. At the end of incubation, the cells were dissociated and washed to stain. We used an FITC Annexin V Apoptosis Detection Kit (BD Biosciences, USA) to detect the apoptosis with the treatment of different prodrugs. These samples were detected by FITC channel and PE channel using FACS Aria. The procedure of detecting the changes of p-Akt (Ser473) was similar before being washed. The dissociated cells were resuspended by stain buffer (BD Biosciences, USA) and fixed by fixation buffer (BD Biosciences, USA). After being washed by stain buffer for 3 times, the cells were treated by perm buffer III (BD Biosciences, USA). Then the cells were stained by PE mouse anti-Akt (pS473) and relative isotype control (BD Biosciences, USA) to evaluate the level of phosphorylation of the cells through FACS Aria (BD Biosciences, USA).

Mice: All animal experiments were performed in accordance with the guidelines established by the Committee of Animal Research Policy of Binzhou Medical University. 5-week-old female specific pathogen free (SPF) athymic nude mice and BALB/c mice were obtained from Changzhou Cavens Lab Animal Co. Ltd. The animals were housed in individual ventilated cages and fed a SPF laboratory diet and water *ad libitum*. 2×10^6 cells were suspended in media and implanted subcutaneously into nude mice.

Histological experiments: Lungs and tumors from nude mice were excised. The tissues were fixed in 10% formaldehyde and embedded in paraffin. Then the paraffin masses were cut and dewaxed. The sections were dehydrated using graded ethanol series and washed by ultrapure water. The lung sections were stained with hematoxylin and eosin to observe the pulmonary tissue structure. Immunofluorescence staining followed the dehydration. After being treated with Triton X-100 and serum, the sections were stained by Ki-67 (D3B5) Rabbit mAb (Alexa Fluor® 647 Conjugate) (Cell Signaling Technology, USA)

overnight. The sections were stained by DAPI to display the nucleus and enveloped by glycerol before observation.

Imaging mice *in vivo*: A *In-vivo* Imaging System was employed to image nude mice treated by TPG, TBG or Probe-PA. The excitation and emission wavelengths were chosen as described in paper. The mice were anesthetized prior to injection and during imaging. After *in vivo* imaging, the organs (lung, heart, liver, kidney and spleen) and tumors were excised to perform *ex vivo* imaging.

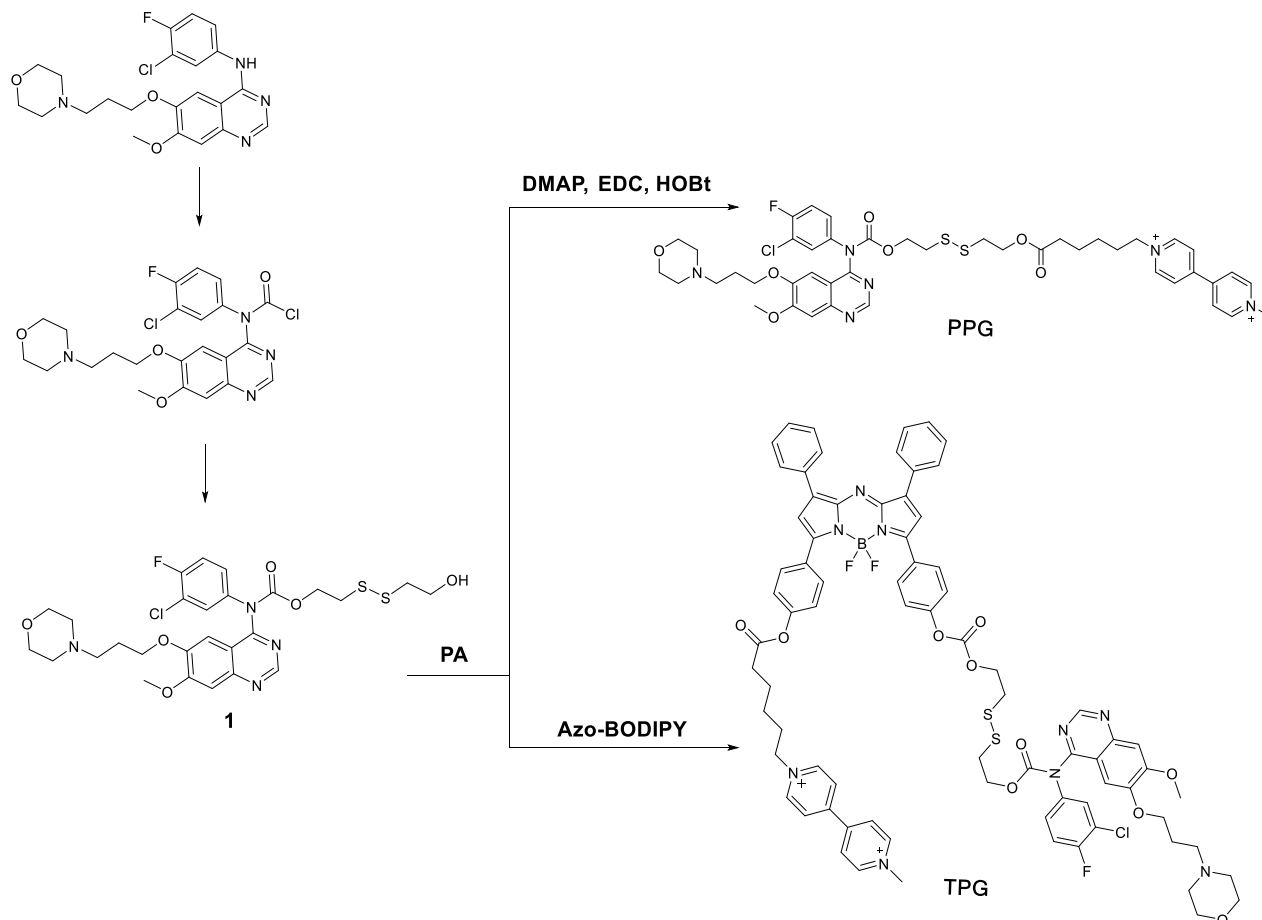
Patient samples: TBLB tissues were obtained from Department of Respiratory Medicine, Affiliated Hospital of Binzhou Medical University. CT scanning was taken before TBLB to ensure the suspected locations. Informed written consents were provided by all patients. The experiments were approved by the Ethics Committee of Binzhou Medical University.

Cancer cells detection of clinical tissues: The TBLB tissues were separated under the direct vision and placed into 10 mL cold Hank's Balanced Salt Solution (HBSS) (Gibco, USA). The tissues were cut into pieces as small as possible and washed three times by HBSS. 200 U/mL type I collagenase (Gibco, USA) HBSS solution were made and heated to 37°C. The small tissues were placed into the collagenase solution at 37°C for 3 h, in order to obtain the single cell suspension. The screen mesh was used to filter the cell masses and the collagenase was discarded by centrifuge. The cells were washed by PBS three times and treated by FACS Lysing Solution (BD Bioscience, USA). The cells were washed three times and counted to suspend by 1 mL RMPI-1640 medium. 5 µM TPG was added into the single cell suspension to stain for 15 min at 37°C. After being washed by PBS twice, the cells were treated by ice ethanol at -20°C overnight. At the end of last procedure, CEA Antibody, FITC (CI-P83-1) (Invitrogen, USA) and Cytokeratin 19 Monoclonal Antibody (A53-B/A2), Alexa Fluor 488 (Invitrogen, USA) were used to stain the cells for 30 min. After being washed three times, the cells were counted and tested with flow cytometry with a collection of 10⁴ cells.

Statistical analysis: Statistical Product and Service Solutions (SPSS) software 19.0 was used for the statistical analysis. The error bars shown in the figures represented the mean ± s.d. Differences were determined with a one-way, two-way analysis of variance (ANOVA) followed by LSD test. Differences between two groups were assessed by using the Student's *t*-tests. Statistical significance was assigned at **P* < 0.05, ***P* < 0.01. Sample size was chosen empirically based on our previous experiences and pre-test results. No statistical method was used to predetermine sample size and no data were excluded. The numbers of animals or samples in every group were described in the corresponding figure legends. The distributions of the data were normal. All experiments were done with at least three biological replicates. Experimental groups were balanced in terms of animal age, sex and weight. Animals were all caged together and treated in the same way. Appropriate tests were chosen according to the data distribution. Variance was comparable between groups in experiments described throughout the manuscript.

Investigator was not blinded to the group allocation during the experiment or to outcome assessments. No randomization was used to allocate animals to experimental groups.

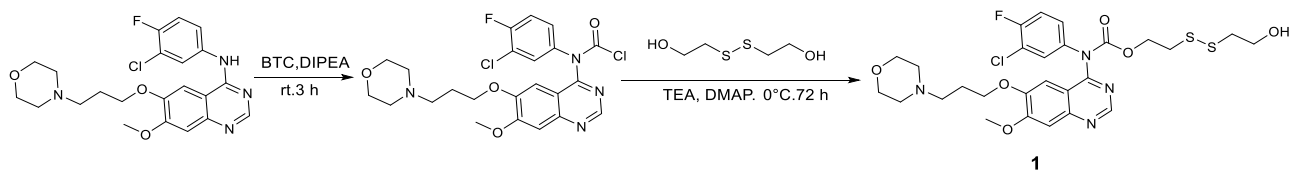
2. Synthesis and Characterization of Compounds



Scheme S1 The synthesis routes of PPG and TPG.

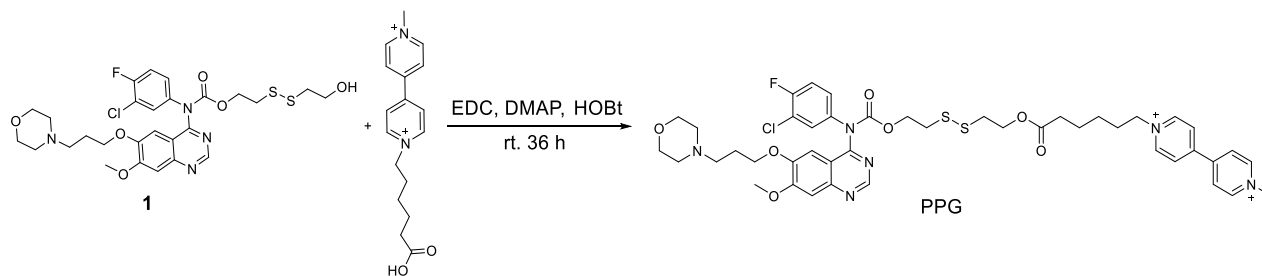
Synthesis of Compound 1. The Gefitinib (0.116 g, 0.26 mmol) was dissolved into 100 mL dichloromethane (DCM) in an ice bath. When the tiphosgene (1.539 g, 5.2 mmol) was dissolved into the solution, N,N-diisopropylethylamine (DIPEA) (1.006 g, 7.8 mmol) in 10 mL DCM was dropwise added into the mixture. At the end of the process of dropping, the mixture was heated at room temperature for 3 h under argon atmosphere. The mixture was evaporated to obtain yellow solid and dropped into an anhydrous tetrahydrofuran (THF) solution containing 2-hydroxyethyl disulfide (0.200 g, 1.3 mmol), triethylamine (0.788 g, 0.78 mmol) and 4-dimethylaminopyridine (DMAP) (catalytic) at 0°C under argon atmosphere. The reaction was stirred for 72 h at 0°C and stopped by adding water to the mixture. After evaporated, re-dissolved solvent with 200 mL DCM was washed by brine (200 mL × 3). The organic layer was dried by sodium sulphate and filtered. The solvent was evaporated and purified by

silica gel column chromatography using DCM/MeOH (30:1, v/v) as eluent to afford Compound 1 (0.101 g, yield: 62%) as yellow white solid.



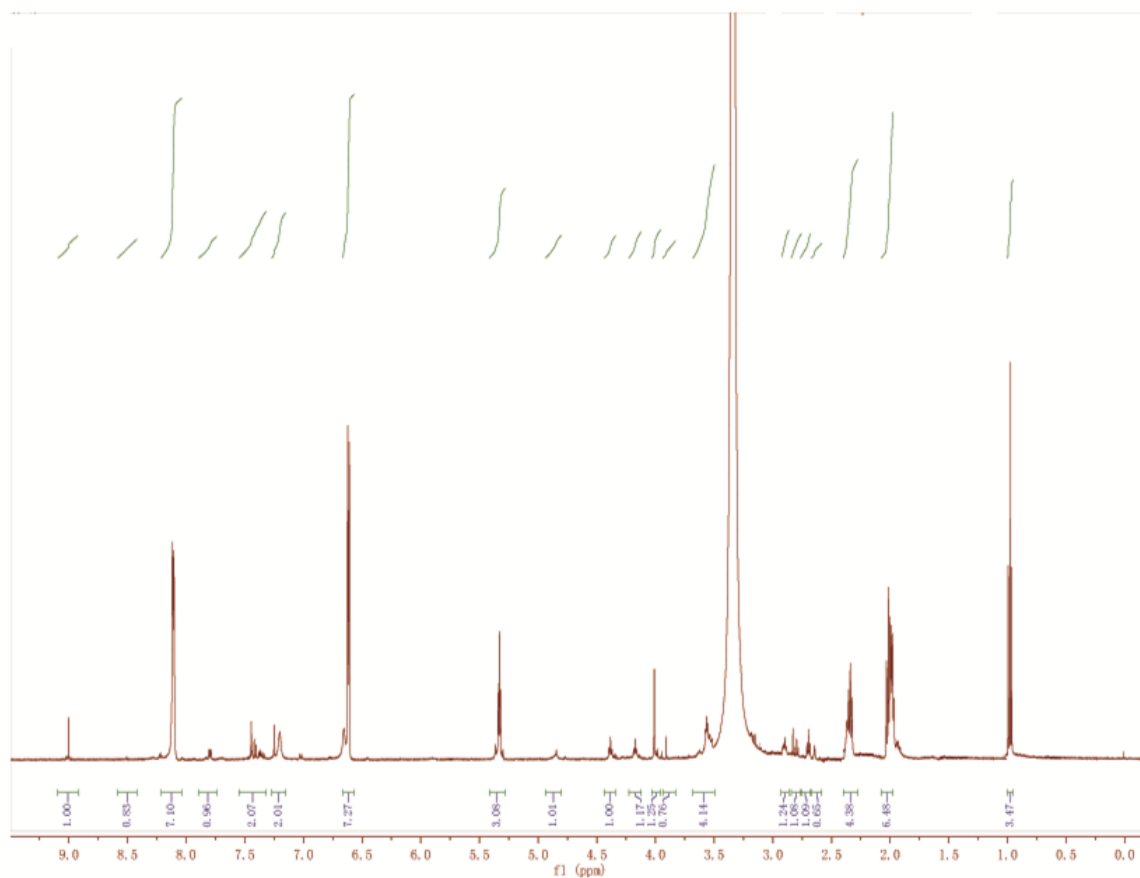
Compound 1: ^1H NMR (DMSO- d_6 , 500 MHz) δ (ppm) 9.03 (s, 1H), 8.99 (s, 1H), 7.79 (d, 1H), 7.45 (s, 1H), 7.43 (s, 1H), 7.32 (s, 1H), 4.93 (s, 1H), 4.36 (s, 2H), 4.24 (s, 2H), 4.01 (s, 3H), 3.92 (s, 4H), 3.52 (s, 2H), 3.17 (d, 4H), 2.88 (s, 2H), 2.69 (s, 2H), 2.50 (s, 2H), 2.31 (s, 2H). ^{13}C NMR (DMSO- d_6 , 125 MHz) δ (ppm) 158.11, 156.91, 155.31, 153.63, 150.90, 150.41, 137.75, 132.14, 132.04, 129.65, 129.15, 128.20, 120.11, 119.97, 117.73, 117.56, 117.40, 107.26, 103.30, 67.12, 64.68, 63.67, 59.69, 57.10, 54.03, 51.55, 49.18, 41.53, 36.99, 30.48, 29.48, 19.06, 14.05, 11.62. LC-MS (ESI $^+$): m/z $\text{C}_{27}\text{H}_{32}\text{ClFN}_4\text{O}_6\text{S}_2$ calcd. 626.1436, found $[\text{M}+\text{H}]^+$ 627.1506.

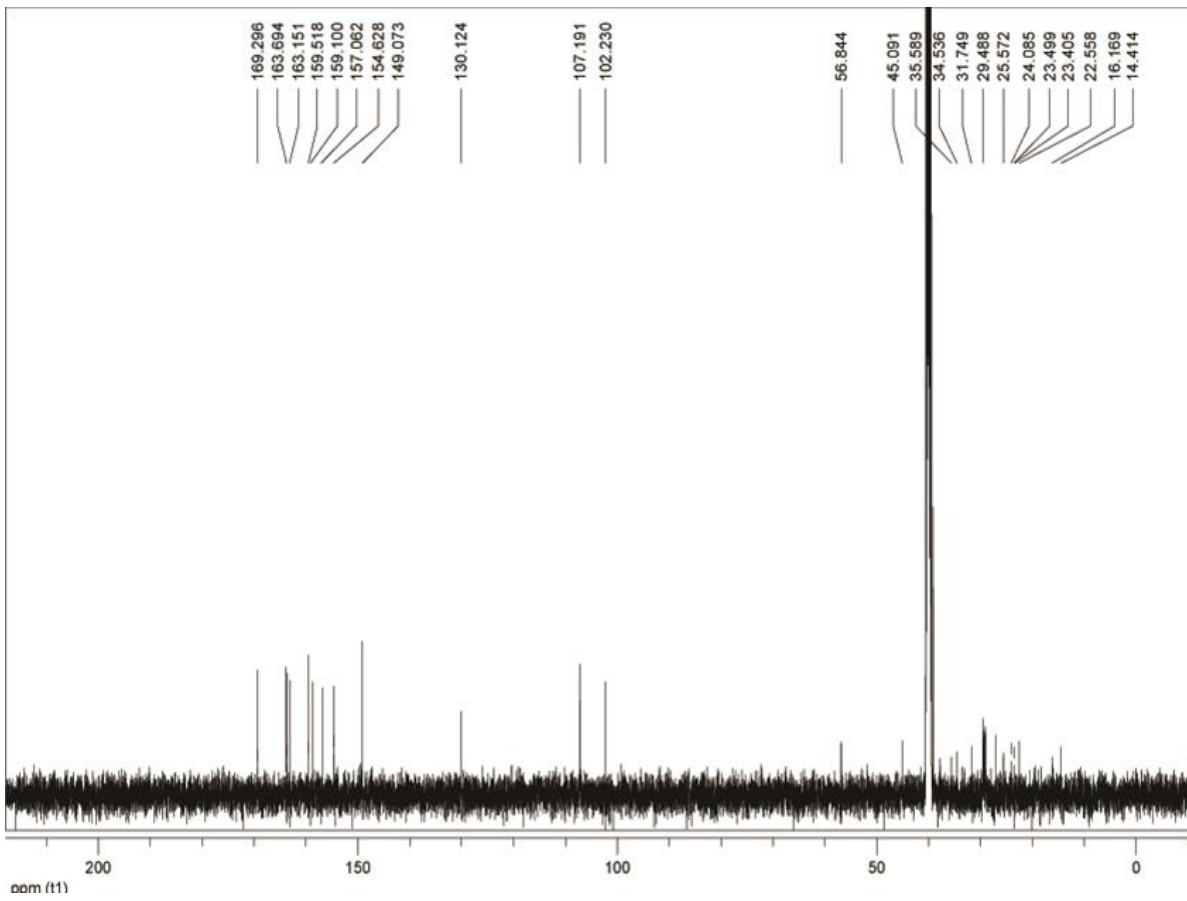
Synthesis of Prodrug Polyamine Analogue-Gefitinib (PPG). The synthesis route of PA was reported by the previous work.¹ PA (0.197 g, 0.4 mmol) was dissolved into 50 mL N,N-dimethylformamide (DMF). 1-(3-Dimethylaminopropyl) -3-ethylcarbodiimide hydrochloride (EDC) (0.092 g, 0.48 mmol), DMAP (0.048 g, 0.4 mmol) and 1-hydroxybenzotriazole (HOBt) (catalytic) was added into the solution stirring for 30 min at room temperature.² Compound 1 (0.125 g, 0.2 mmol) was added dropwise in the above solution. The reaction was stirred for 24 h and stopped by adding water. The obtained mixture was extracted with DCM (200 mL \times 3) and brine (200 mL \times 3). The organic layer was dried over anhydrous sodium sulphate for 8 h and filtered through a Buchner funnel to obtain the solution. The solvent was evaporated in vacuum. Then re-dissolved with DCM and purified with aluminium oxide column chromatography with the eluent of DCM/MeOH (40:1, v/v), obtaining PPG (0.093 g, yield: 42%).



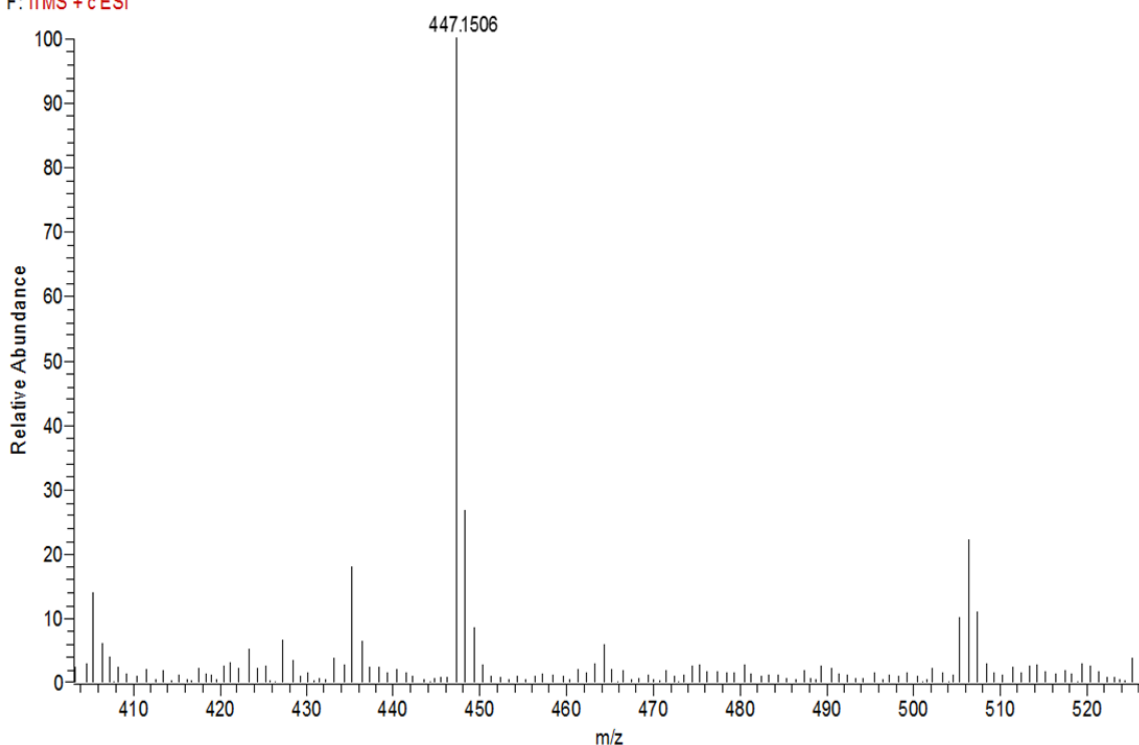
PPG: ^1H NMR (500 MHz, DMSO- d_6) δ (ppm): 8.99 (s, 1H), 8.51 (s, 1H), 8.15-8.10 (m, 7H), 7.80-7.78 (m, 1H), 7.44-7.34 (m, 2H), 7.24-7.20 (m, 2H), 6.70-6.58 (m, 7H), 5.33 (m, 3H), 4.84 (s, 1H), 4.39-4.33 (m, 1H), 4.18-4.15 (t, 1H), 4.00-3.97 (m, 2H), 3.90 (s, 1H), 3.57-3.50 (m, 4H), 2.91-2.89 (m, 1H), 2.82-2.79 (m, 1H), 2.70-2.68 (t, 1H), 2.64-2.63 (m, 1H), 2.38-2.32 (m, 1H), 2.38-2.37 (t, 4H), 2.06-1.95 (m,

6H), 1.00-0.94 (m, 3H). ^{13}C NMR (125 MHz, DMSO- d_6) δ (ppm): 169.29, 163.69, 163.15, 159.52, 159.10, 157.06, 154.62, 149.07, 130.12, 107.19, 102.23, 56.84, 45.09, 35.59, 34.53, 31.75, 29.48, 25.57, 24.08, 23.50, 23.40, 22.56, 16.17, 14.41. LC-MS (ESI $^+$): m/z $\text{C}_{44}\text{H}_{52}\text{ClFN}_6\text{O}_7\text{S}_2^{2+}$ calcd. 894.3000, found $[\text{M}^{2+}]$ 447.1506.

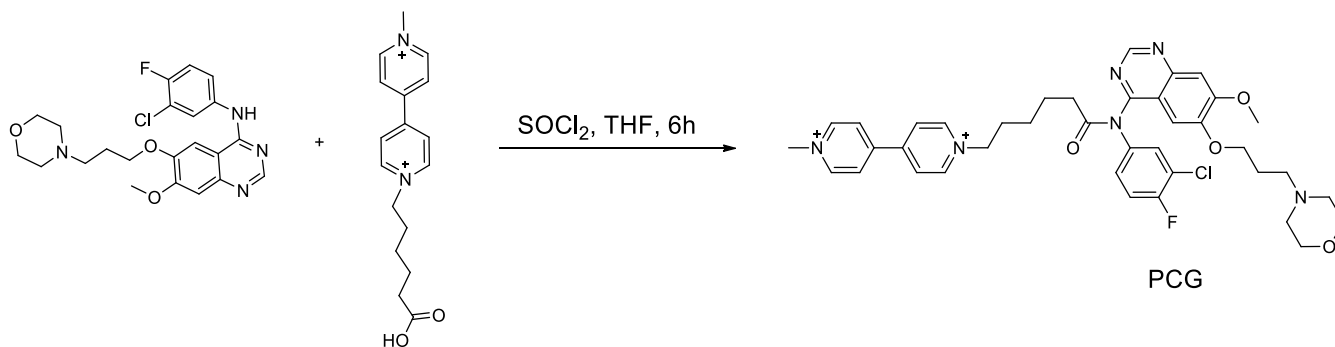




SXY-SP-1227#13-58 RT: 0.18-0.63 AV: 23 NL: 1.83E4
F: ITMS + cESI



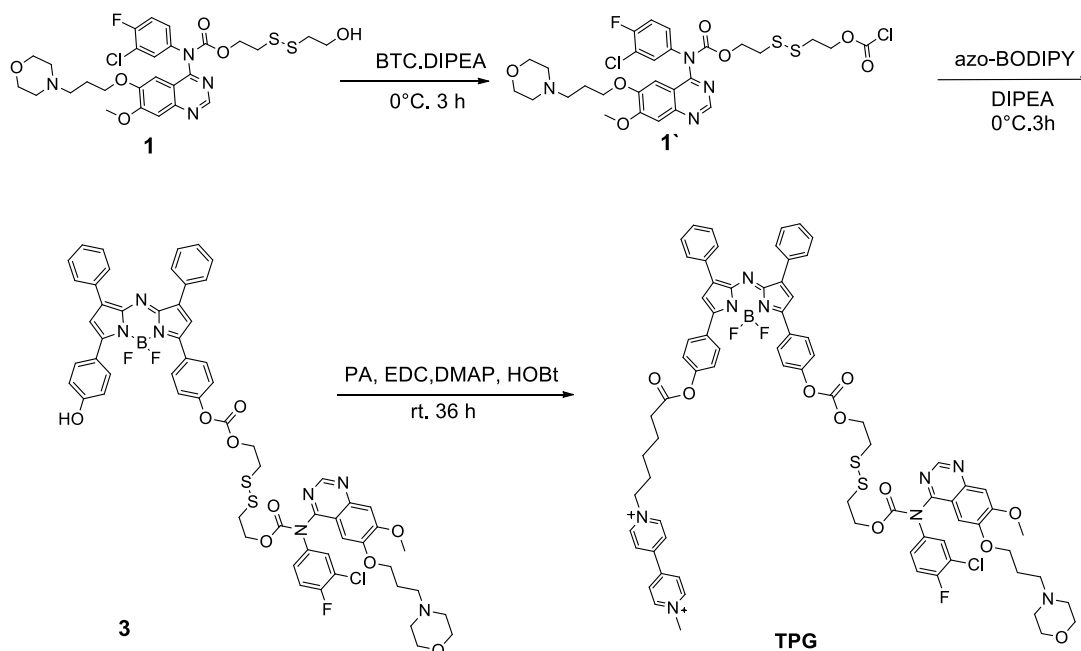
Synthesis of Compound PCG. PA (0.197 g, 0.4 mmol) was dissolved into 50 mL anhydrous tetrahydrofuran (THF) and 2 mL SOCl₂. After refluxed 1 h, the solvent was evaporated in vacuum. The remaining solid was dissolved with 50 mL THF. Gefitinib (0.116 g, 0.26 mmol) was added. The reaction was lasted for 10 h at 0 °C and then refluxed for more 5 h. After evaporated solvent, the residue was dissolved with DCM and purified with aluminium oxide column chromatography with the eluent of DCM/MeOH (40:1, v/v), obtaining Compound 2 (0.123 g, yield: 60%).



Compound PCG: ¹H NMR (500 MHz, DMSO-d₆) δ (ppm): 9.01-9.03 (d, 4H), 8.96-8.93 (m, 5H), 7.88-7.87 (m, 1H), 7.54-7.35 (m, 4H), 5.39 (m, 3H), 4.03-3.99 (t, 2H), 3.89 (s, 3H), 3.54-3.50 (m, 4H), 2.90-2.88 (t, 2H), 2.43-2.31 (m, 8H), 2.05-1.94 (m, 4H), 1.05-0.99 (m, 4H). ¹³C NMR (125 MHz, DMSO-d₆) δ (ppm): 170.10, 163.89, 163.25, 159.51, 159.11, 157.08, 154.65, 150.01, 149.02, 129.92, 107.21,

106.53, 58.84, 53.09, 45.39, 35.61, 35.13, 28.27, 28.18, 23.53, 22.49. LC-MS (ESI⁺): m/z C₄₄H₅₂ClFN₆O₇S₂²⁺ calcd. 714.3086, found [M²⁺] 357.1541.

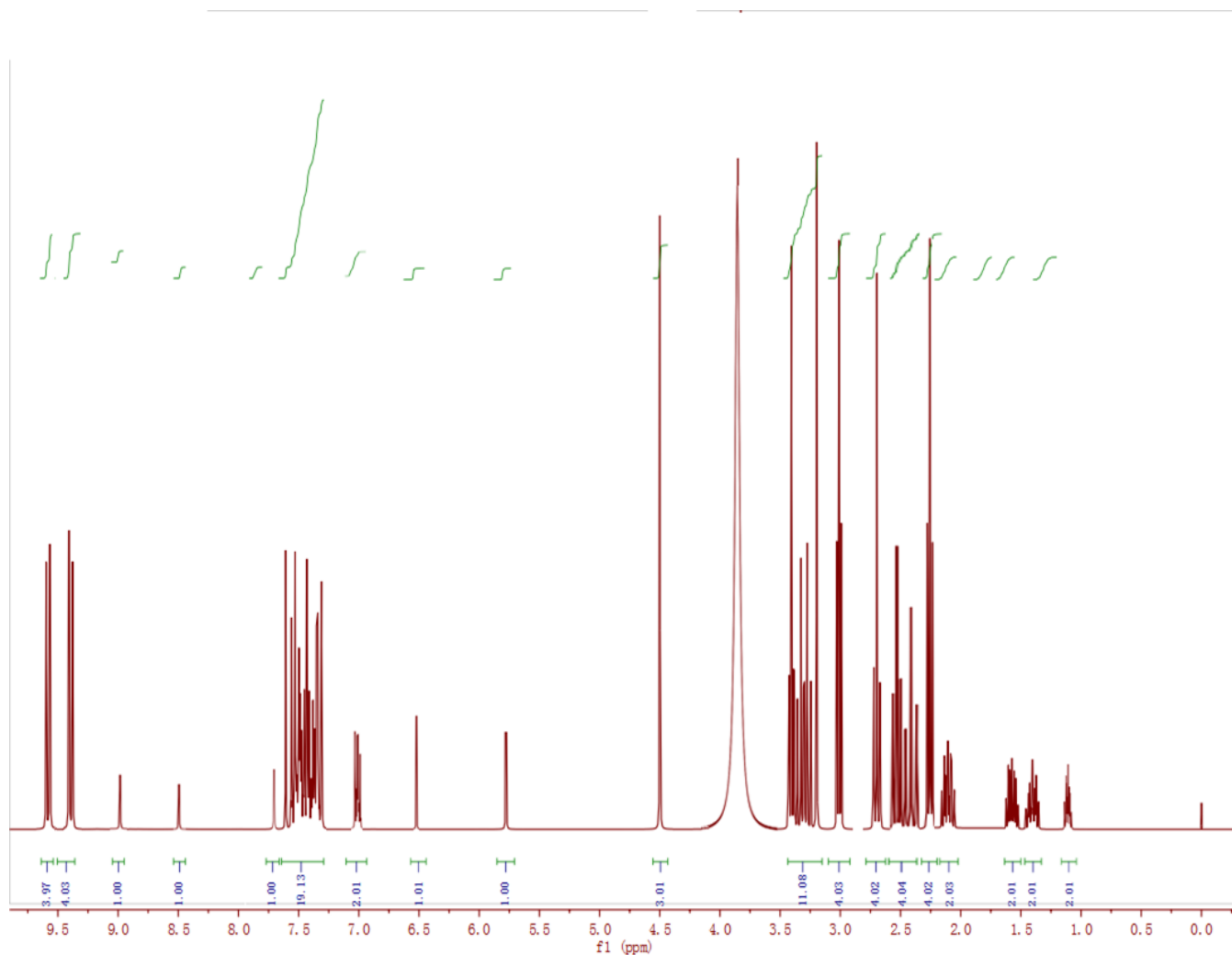
Synthesis of Theranostics Polyamine Analogue-Gefitinib (TPG). The synthesis route of *azo*-BODIPY was reported by the previous work.³ Compound 1 (0.194 g, 0.31 mmol) and triphosgene (1.835 g, 6.2 mmol) were dissolved in a 250 mL round bottom flask with 100 mL DCM and DIPEA (1.200 g, 9.3 mmol) was dropped into the solution under argon atmosphere at ice bath. The reaction was stirred for 3 h at room temperature and the solvent was evaporated. The re-dissolved solvent with 10 mL DCM was added dropwise into the 50 mL DCM solution containing DIPEA (0.040 g, 0.31 mmol) and *azo*-BODIPY (0.132 g, 0.25 mmol) under argon atmosphere at room temperature. The reaction was stirred for 36 h at room temperature and was stopped with adding water. The crude was extracted with DCM (200 mL × 3) and brine (200 mL × 3) and the organic layer was dried with sodium sulphate for 8 h. The solvent was evaporated and purified through aluminium oxide column chromatography with the eluent of DCM/MeOH (40:1, v/v) to obtain Compound 2 (0.145 g, yield: 49%) as bluegreen solid. PA (0.246 g, 0.5 mmol) was dissolved into 50 mL DMF and EDC (0.115 g, 0.6 mmol), DMAP (0.061 g, 0.5 mmol) and HOBT (catalytic) were added into the solution stirring for 30 min at room temperature. Compound 2 (0.118 g, 0.1 mmol) was added dropwise in the above solution. The reaction was stirred for 36 h and evaporated with the oil pump to acquire the solid. The solid was washed by DCM with a Buchner funnel to obtain the blue solid, TPG (0.030 g, yield: 18%).

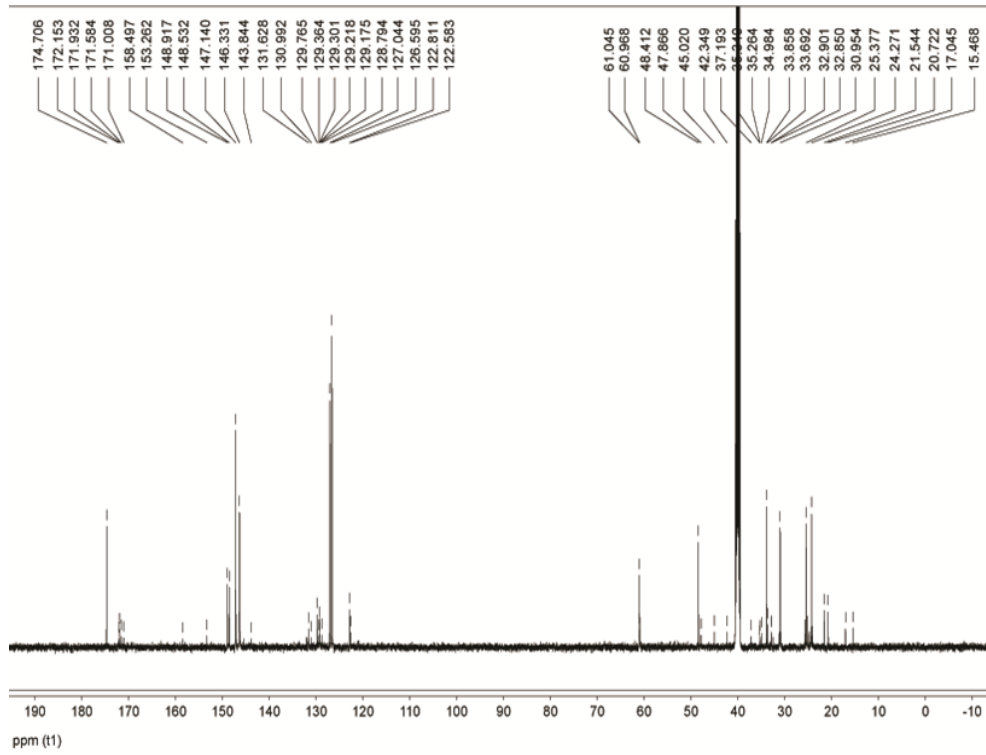


Compound 3: ¹H NMR (500 MHz, DMSO-d₆) δ (ppm): 12.08 (s, 1H), 9.59-9.52 (m, 5H), 9.41-9.40 (d, 5H), 8.91-8.87 (m, 10H), 8.20-8.11 (m, 2H), 7.57-7.36 (m, 4H), 4.78-4.75 (t, 4H), 3.25-3.134 (m, 1H), 2.72-2.68 (m, 1H), 2.32-2.23 (m, 4H), 2.02-1.99 (t, 4H), 1.58-1.55 (m, 4H), 1.35-1.32 (m, 4H), 1.12-

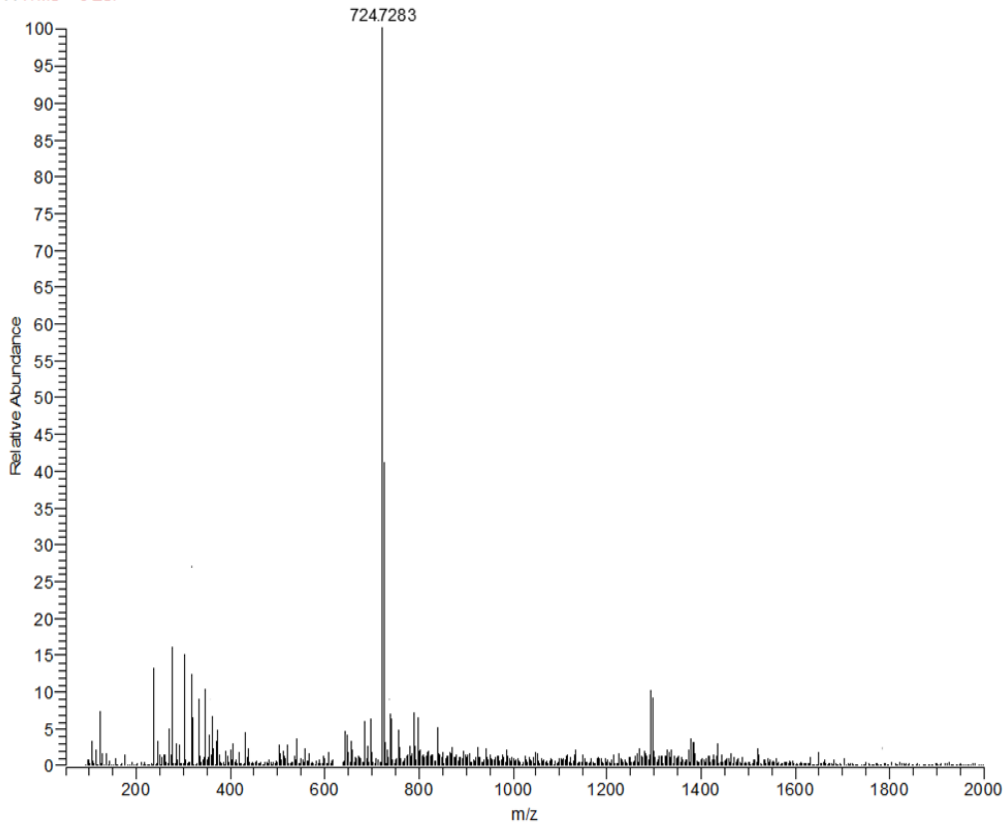
0.99 (m, 3H). ^{13}C NMR (125 MHz, DMSO- d_6) δ (ppm): 174.70, 171.01, 158.50, 153.26, 148.92, 148.53, 147.14, 146.33, 132.04, 131.62, 130.99, 129.76, 129.30, 127.04, 126.59, 122.81, 60.96, 48.41, 47.86, 45.02, 42.35, 37.19, 34.98, 33.86, 30.59, 25.38, 24.27, 21.54, 20.72, 17.04, 15.46. LC-MS (ESI $^+$): m/z $\text{C}_{60}\text{H}_{52}\text{BClF}_3\text{N}_7\text{O}_9\text{S}_2$ calcd. 1181.3002, found $[\text{M}+\text{H}]^+$ 1182.3074.

TPG: ^1H NMR (DMSO- d_6 , 500 MHz) δ (ppm) 9.67 – 9.48 (m, 4H), 9.41-9.40 (m, 4H), 8.94 (s, 1H), 7.84 (s, 1H), 7.67 (s, 1H), 7.58 – 7.32 (m, 19 H), 7.05-7.04 (m, 2H), 6.52(s, 1H), 5.77 (s, 1H), 4.50 (s, 3H), 3.37 – 3.19 (m, 11H), 3.08-2.95 (m, 4H), 2.72 – 2.69 (m, 4H), 2.61 – 2.21 (m, 8H), 2.15 – 1.93 (m, 2H), 1.59-1.53 (m, 2H), 1.47 – 1.31 (m, 2H), 1.12 – 1.10 (m, 2H). ^{13}C NMR (DMSO- d_6 , 125 MHz) δ (ppm) 174.71, 172.15, 171.93, 171.58, 158.49, 153.26, 149.59, 148.92, 148.53, 147.50, 147.14, 146.33, 131.63, 130.99, 129.77, 129.36, 129.30, 129.21, 129.30, 129.17, 128.79, 127.04, 126.60, 122.81, 122.58, 61.04, 60.97, 48.41, 47.87, 45.02, 42.35, 37.19, 35.34, 34.98, 33.85, 33.69, 32.90, 32.85, 30.95, 25.37, 24.24, 21.54, 20.72, 17.04, 15.46. LC-MS (ESI $^+$): m/z $\text{C}_{77}\text{H}_{72}\text{BClF}_3\text{N}_9\text{O}_{10}\text{S}_{22}^{2+}$ calcd. 1449.4566, found $[\text{M}]^{2+}$ 724.7283.





S11251_151125145235 #14-26 RT: 0.17-0.32 Av: 7 NL: 6.35E4
 F: ITMS + c ESI



4. Mechanism of TPG releasing Gefitinib and emitting NIR fluorescence

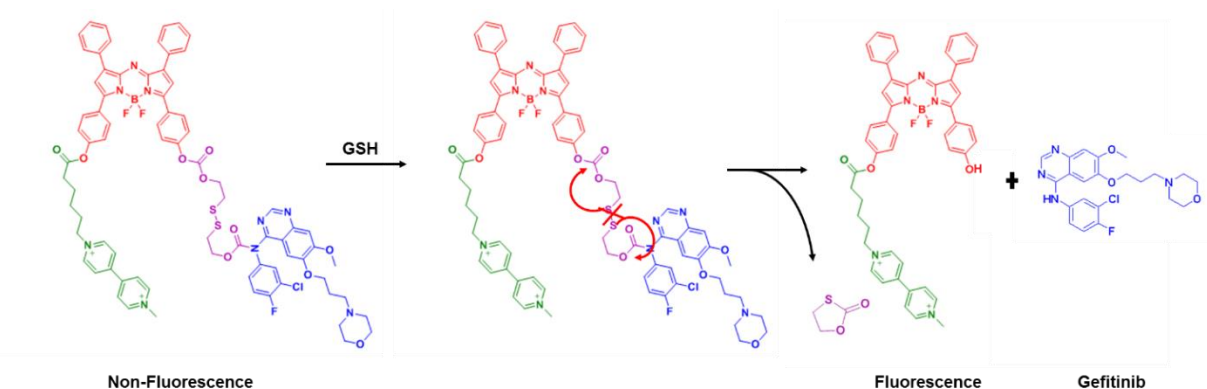


Figure S2. Mechanism of Gefitinib released and NIR fluorescence emitting by the reaction between GSH and TPG.

5. Spectral properties and selectivity of TPG towards GSH

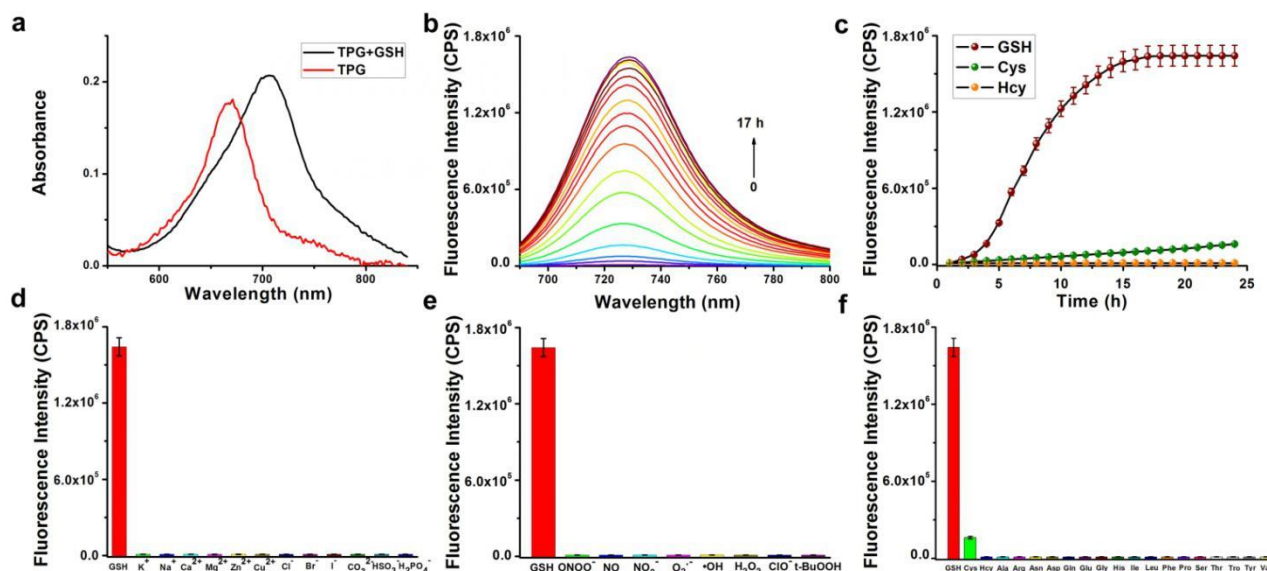


Figure S3. Spectral dynamics of TPG towards GSH. All the spectra experiments were accomplished in 10 mM HEPES buffer (pH 7.4, 0.5% DMSO, 0.4% Tween 80) at 37°C. (a) Absorbance spectra of TPG towards GSH. The absorbance of TPG (10 μ M) (red) and TPG incubated with GSH (10 mM) (black) was measured. (b) Time-dependent fluorescence intensity upon treatment of GSH (10 mM). (Channel: $\lambda_{ex/em} = 706/690-800$ nm) (c) Time dependent fluorescence intensity at 730 nm of TPG (10 μ M) towards GSH (10 mM), cysteine (Cys) (200 μ M) and homocysteine (Hcy) (10 μ M) during 0 – 24 h. GSH, Cys and Hcy were added at the start of reaction and the reactions were measured during 0 – 24 h. (Channel: $\lambda_{ex/em} = 706/730$ nm) (d) Selectivity of TPG toward anions and metal ions. The fluorescence intensities were measured after the following substances reacting with TPG for 24 h. 10 mM GSH; 5 mM K^+ ; 140 mM Na^+ ; 2.5 mM Ca^{2+} ; 1 mM Mg^{2+} ; 1 mM Zn^{2+} ; 1 mM Cu^{2+} ; 1 mM Cl^- ; 1 mM Br^- ; 1 mM I^- ; 1 mM CO_3^{2-} ; 1 mM HSO_3^- ; 1 mM $H_2PO_4^-$. (e) Selectivity of TPG toward reactive oxygen species and reactive nitrogen species. The fluorescence intensities were measured after the following substances reacting with TPG for 24 h. 10 mM GSH; 200 μ M ONOO $^-$; 200 μ M NO; 200 μ M NO_2^- ; 200 μ M O_2^- ; 200 μ M $\cdot OH$; 200 μ M H_2O_2 ; 200 μ M ClO $^-$; 200 μ M *t*-BuOOH. (f) Selectivity of TPG toward amino acids and peptides. The fluorescence intensities were measured after the following substances reacting with TPG for 24 h. 10 mM GSH; 200 μ M Cys; 10 μ M Hcy; 1 mM Ala; 1 mM Arg; 1 mM Asn; 1 mM Asp; 1

mM Gln; 1 mM Glu; 2 mM Gly; 1 mM His; 1 mM Ile; 1 mM Leu; 1 mM Phe; 1 mM Pro; 1 mM Ser; 1 mM Thr; 1 mM Tro; 1 mM Tyr; 1 mM Val. The experiments were repeated three times and the data were shown as mean (\pm s.d.).

6. Reaction kinetics of prodrug and GSH monitored by HPLC.

In order to verify that prodrug (PPG) could release Gefitinib without the interference of *azo*-BODIPY. We carried out the inspection of reaction kinetics between prodrug and GSH by reversed-phase high performance liquid chromatography (RP-HPLC). Samples were separated on RP-HPLC with a ZORBAX SB-C18 column (4.6 \times 150 mm, 5 μ m), acetonitrile/0.15% (v/v) ammonium acetate (adjusted pH 8.0 with ammonium hydroxide) =(85:15, v/v) as mobile phase at a flow rate of 1.0 mL/min, detection wavelength of 310 nm and column temperature of 37 $^{\circ}$ C, injection volume: 20 μ L. GSH (10 mM) was used to cleave the disulfide of prodrug (10 μ M). As shown in Figure S4a, the peak of PPG appeared at 2.06 min when the reaction started. The peak at 2.41 min representing Gefitinib gradually rose. The reaction stopped at the end of 17 h. This indicated a consistent result of spectral dynamics. As shown in Figure S4b, the cumulative release of PPG was further quantified according to HPLC in Figure S4a.

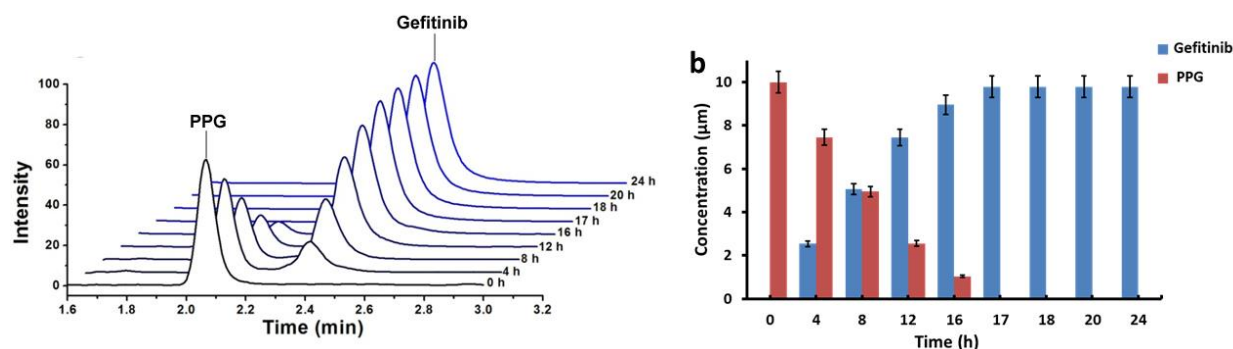


Figure S4 (a) Reaction kinetics of the reaction between PPG and GSH monitored by HPLC. GSH (10 mM) was added into PPG (10 μ M) at the start of reaction and the reactions were measured during 0 – 24 h. (b) The cumulative release of PPG was further quantified according to HPLC result.

7. Time-dependent fluorescence intensity of TPG in PC9 cells and H1650 cells.

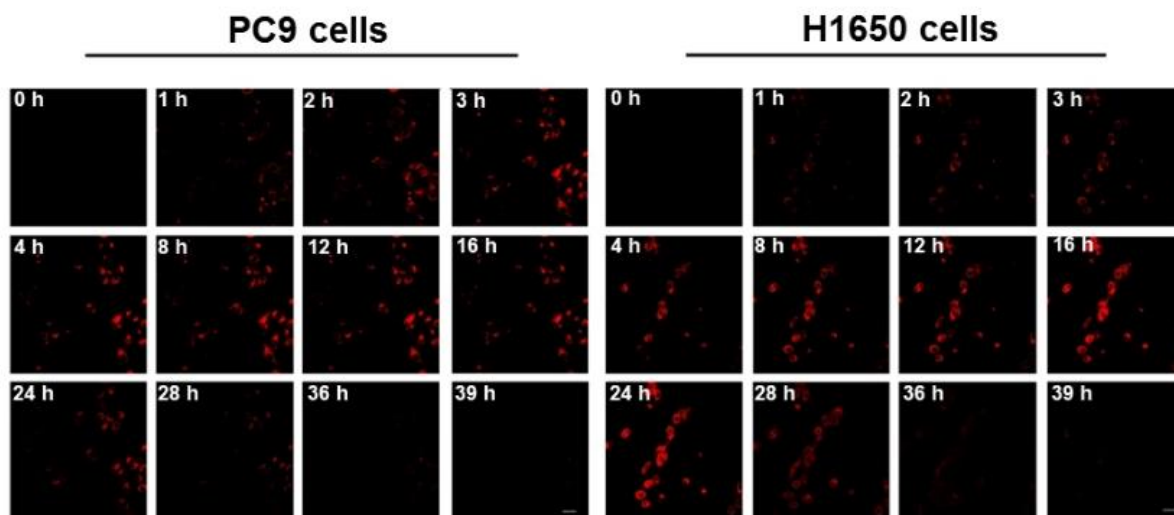


Figure S5. Time-dependent fluorescence intensity of TPG in PC9 cells and H1650 cells. Fluorescent images of PC9 cells and H1650 cells treated with 1 μ M TPG for different hours with confocal laser scanning microscope. Channel: $\lambda_{ex/em} = 635/670-770$ nm. Scale bars: 30 μ m.

8. Images of TPG in cysteine treated PC9 cells and H1650 cells

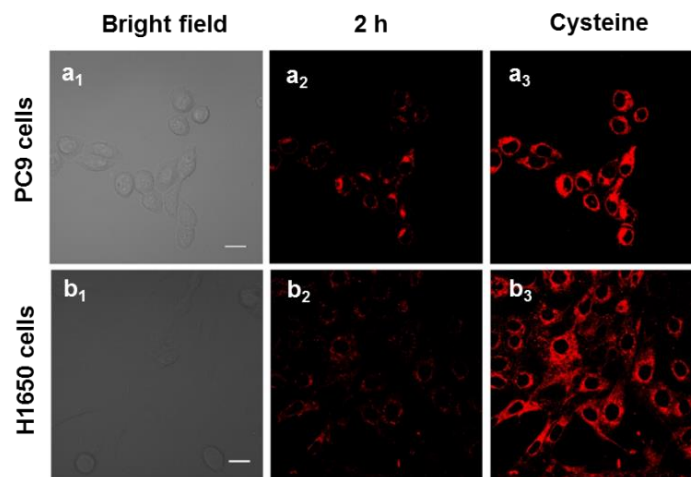


Figure S6. Images of TPG generation in cysteine treated PC9 cells and H1650 cells. PC9 cells and H1650 cells were treated with 1 μ M TPG for 2 h at 37°C and 5 mM cysteine was added into the medium. The images were acquired with confocal laser scanning microscope. Channel: $\lambda_{ex/em} = 635/670-770$ nm. Scale bars: 20 μ m.

9. Images of TPG in NEM treated PC9 cells and H1650 cells

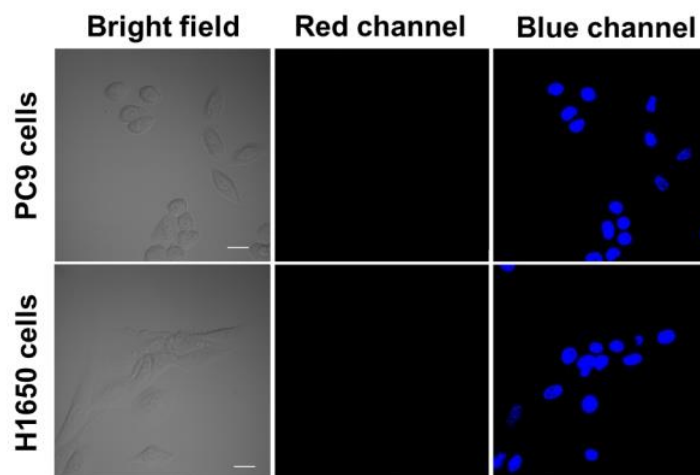


Figure S7. Images of TPG generation in NEM treated PC9 cells and H1650 cells. PC9 cells and H1650 cells were pre-incubated with 5 mM NEM for 30 min at 37°C before exposure to 1 μ M TPG (red channel: $\lambda_{\text{ex/em}} = 635/670-770$ nm) for 2 h. The cells were costained with Hoechst 33258 (blue channel: $\lambda_{\text{ex/em}} = 405/410-490$ nm). The images were acquired with confocal laser scanning microscope. Scale bars: 20 μ m.

10. The investigation of TPG transmembrane transport with corresponding ligand

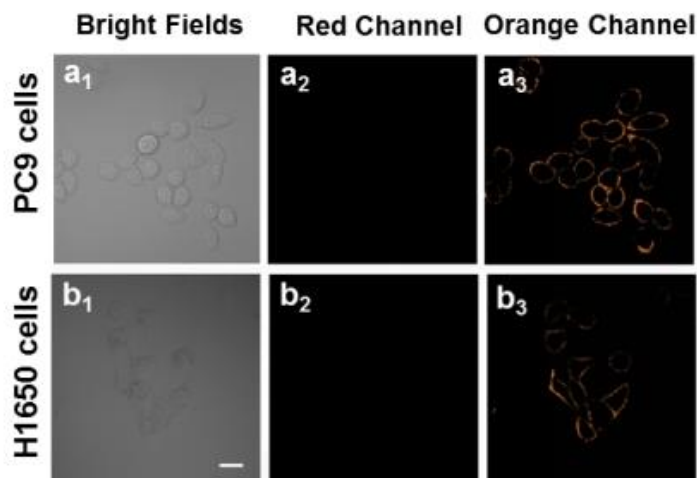


Figure S8. The investigation of TPG transmembrane transport with corresponding ligands. Imaging PC9 cells and H1650 cells treated with 5 μ M PA at 37°C before exposure to 1 μ M TPG (red channel: $\lambda_{\text{ex/em}} = 635/670-770$ nm) for 2 h. The cells were costained with CellMask™ Orange Plasma membrane Stain (orange channel: $\lambda_{\text{ex/em}} = 550/570-630$ nm). Scale bars: 20 μ m.

11. The investigation of TPG transmembrane transport at 4°C

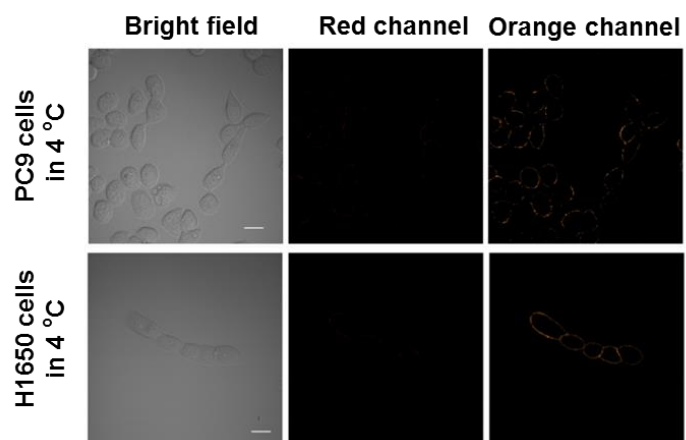


Figure S9. The investigation of TPG transmembrane transport at 4°C. Imaging PC9 cells and H1650 cells placed at 4°C for 1 h before exposed to 1 μ M TPG (red channel: $\lambda_{ex/em}$ = 635/670-770 nm) for 2 h. The cells were costained with CellMask™ Orange Plasma membrane Stain (orange channel: $\lambda_{ex/em}$ = 550/570-630 nm). Scale bars: 20 μ m.

12. Bright-field images of Figure 2a

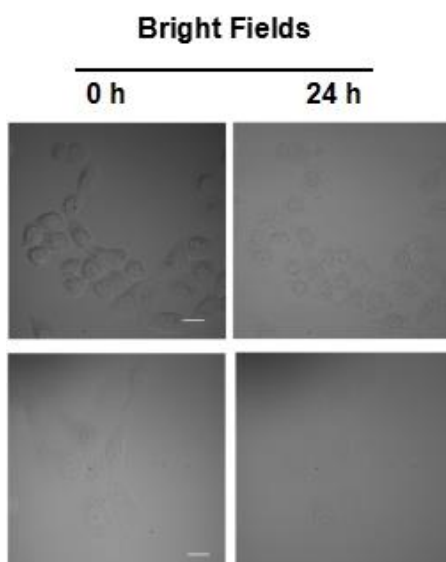


Figure S10. Bright-field images of Figure 2a. Scale bars: 20 μ m.

13. Apoptosis of H1650 cells treated with PA by flow cytometry

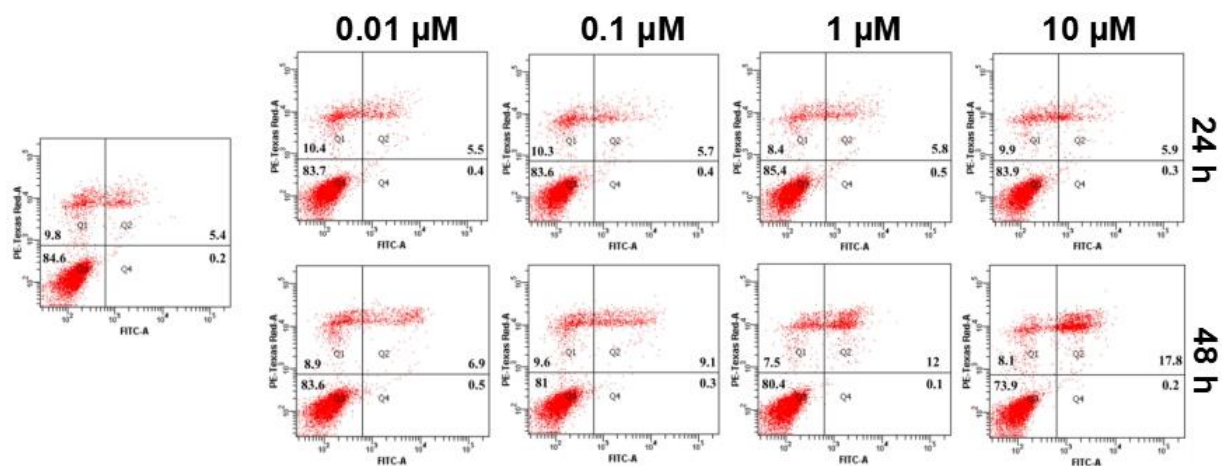


Figure S11. Apoptosis of H1650 cells treated with PA by flow cytometry. H1650 cells were treated with 0.01, 0.1, 1 or 10 μM PA for 24 h or 48 h at 4°C and detected by Annexin V/PI (Q1: necrosis cells, Q2: late apoptotic cells, Q3: survival cells, Q4: early apoptotic cells).

14. Organ targeting of Probe-PA *in vivo* and *ex vivo*

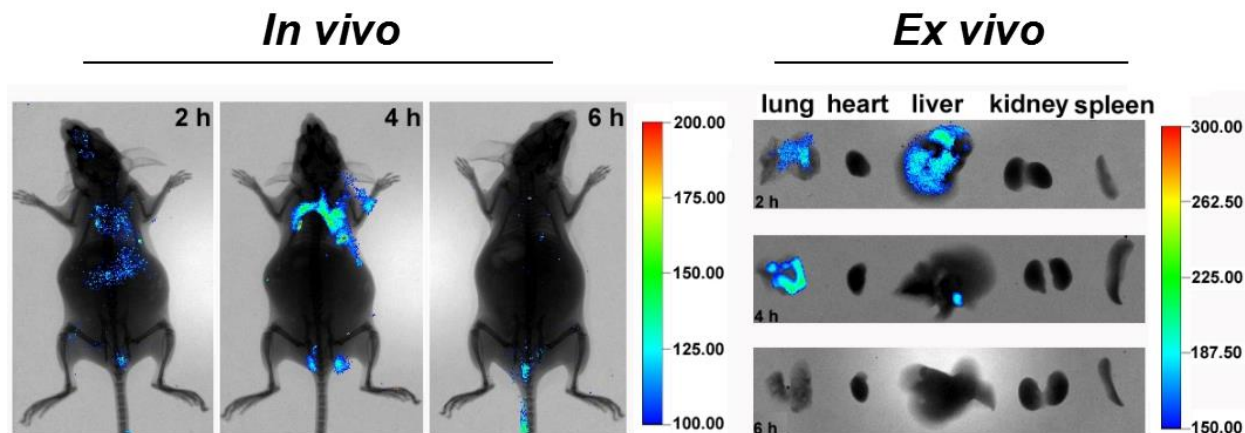


Figure S12. Organ targeting of Probe-PA *in vivo* and *ex vivo*. BALB/c mice were injected via tail vein with a single-dose 0.2 mL of Probe-PA (1 mM) (DMSO/saline 1:1/v/v) and imaging after 2, 4 and 6 h. Separated organs (lung, heart, liver, kidney, spleen) of the mice were also imaged.

15. Fluorescence distribution of TPG and TBG in PC9 and H1650 tumor

The fluorescent images were used to prove the fluorescence distribution of TPG and TBG in PC9 and H1650 tumor mass. The mice were from those bearing PC9 and H1650 tumors used for efficacy evaluation *in vivo*. The fluorescence mainly accumulated in the tumor tissue, which indicated the drug release occurred in the cell cytoplasm.

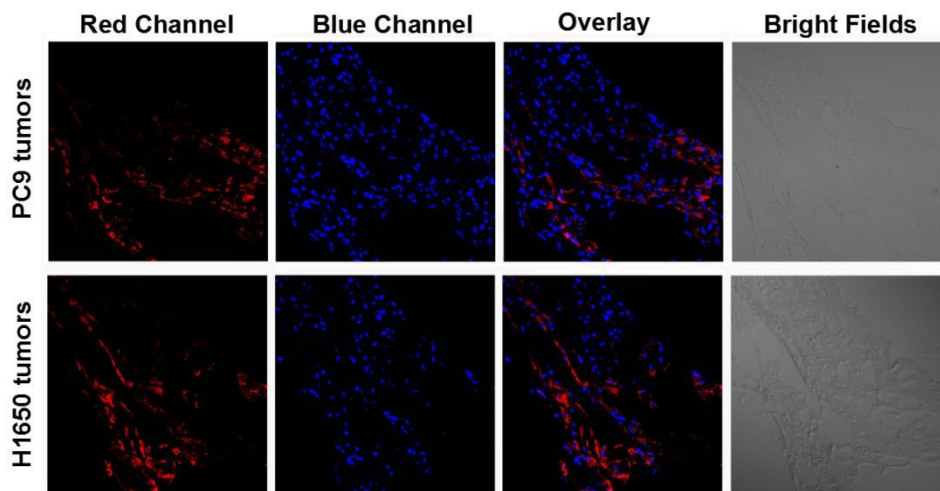


Figure S13. Fluorescence distribution of TPG in PC9 and H1650 tumor. The mice were from those bearing PC9 and H1650 tumors used for efficacy evaluation *in vivo*. The sections were incubated with DAPI for 8 min and imaged with confocal laser scanning microscope. Red channel: $\lambda_{ex/em} = 635/670-770$ nm. Blue channel: $\lambda_{ex/em} = 405/410-490$ nm. Scale bar: 50 μm .

16. Lung sections of the mice treated with the agents

Owing to PA derived from paraquat, we tested the lung toxicity of the treated mice with pathological examination. Compared with the saline group, TPG and PPG groups did not show evidence of pulmonary fibrosis and the capillary congestion was the main change. This indicated that PA indeed accumulated in the lung but could not lead to irreversible lung injury like paraquat.

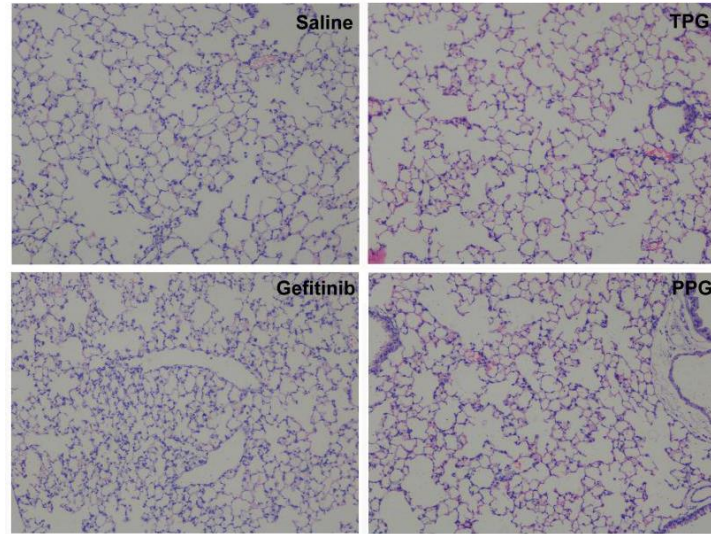


Figure S14. Lung sections of the mice treated with the agents. The mice were from those bearing H1650 tumors used for efficacy evaluation *in vivo*. The lungs were fixed and stained with hematoxylin and eosin. Magnification: $\times 100$.

17. Flow cytometry analysis of TBLB samples

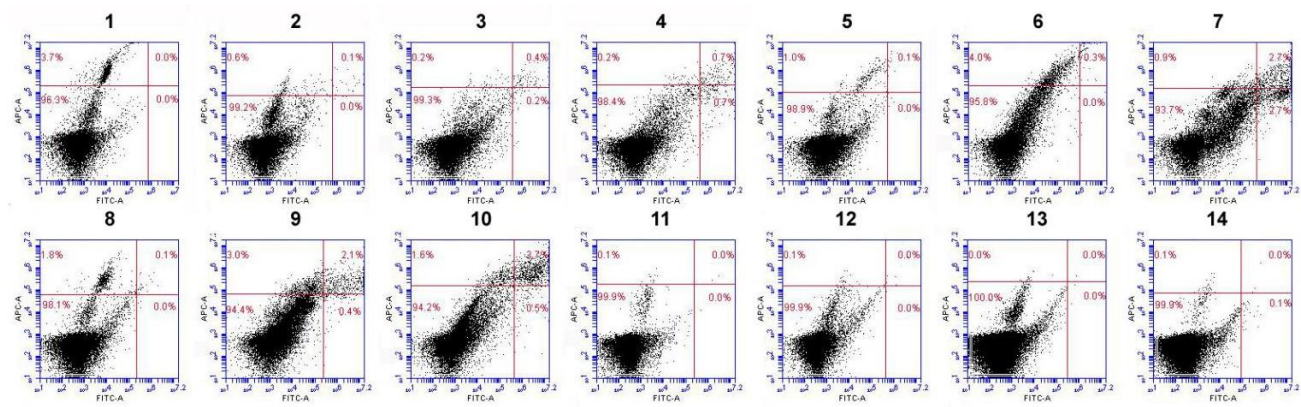


Figure S15. Flow cytometry analysis of TBLB samples. The TBLB tissues were separated under direct vision and dissociated to single cell suspension. APC channel for TPG and FITC channel for CEA and CK19. The numbers were consistent one-to-one matches between Table S1 and Figure S15.

18. Table of the patients` files

Table S1. Table of the patients` files. The clinical data including the sex, age, lesion location, CEA and CK19 in serum, pathological diagnosis and flow cytometry analysis.

No.	Gender	Age	Location	CEA (0-3.4 ng/mL)	CK19 (0.1-3.3 ng/mL)	Diagnosis	Flow cytometry	
							FITC	APC
1	F	64	right lung	1.8	3.6	adenocarcinoma	0	3.7
2	M	66	left lung	2.5	9.4	squamous carcinoma	0.1	0.7
3	F	52	right lung	54.8	1.7	adenocarcinoma	0.6	0.6
4	F	58	right lung	61.7	4.7	adenocarcinoma	1.4	0.9
5	M	63	right lung	3.4	8.5	adenocarcinoma	0.1	1.1
6	F	70	right lung	4.8	9.8	adenocarcinoma	0.3	4.3
7	M	65	right lung	218.3	18.2	squamous carcinoma	5.4	3.6
8	M	86	right lung	1.1	6.0	squamous carcinoma	0.1	1.9
9	M	81	right lung	125.9	48.4	squamous carcinoma	2.5	5.1
10	F	53	left lung	26.5	122.9	adenocarcinoma	4.2	5.3
11	M	53	left lung	-	-	infiltration of chronic inflammation cells	0	0.1
12	M	64	right lung	-	-	infiltration of chronic inflammation cells	0	0.1
13	M	63	left lung	-	-	granulomatous inflammation	0	0
14	F	58	right lung	-	-	infiltration of chronic inflammation cells	0.1	0.1

19. The efficacy of Gefitinib, PA, PPG, as well as a mixture of PA and Gefitinib

To assess the efficacies of Gefitinib, PA, PPG, as well as a mixture of PA and Gefitinib, we employed CCK-8 assay to evaluate their inhibition efficacy in PC9 and H1650 cells, respectively. As shown in Figure S16, the efficacy of PA was not as good as Gefitinib. The CCK-8 results showed that the mixture of PA and Gefitinib could not lead to high PC9 cells inhibition as PPG behaved. But the mixture of PA and Gefitinib caused more inhibition than administration of PA or Gefitinib alone. H1650 was the resistant cell line to Gefitinib. The mixture of PA and Gefitinib could not result in higher inhibition than PPG. The cell viability treated by the mixture of Gefitinib and PA had no significant difference compared with Gefitinib or PA. The low efficacy of PA resulted from the fact that multiple pathways led to tumor occurrence, and single Akt inhibition could not depress the tumor growth.

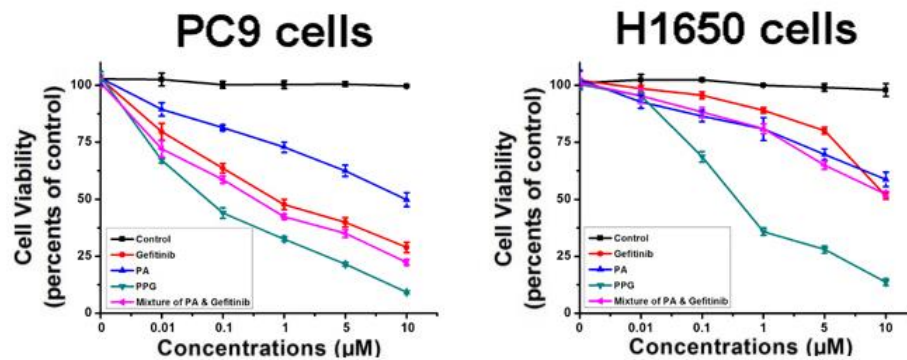


Figure S16. Cell viabilities of PC9 cells and H1650 cells using CCK-8 kit. The cells were treated with Gefitinib, TPG, PPG and a mixture of PA and Gefitinib with 0, 0.01, 0.1, 1, 5 and 10 μM for 72 h, respectively. ($n = 6$ independent experiments).

20. The efficacy assay of control prodrug PCG

To evaluate the efficacy and the response to thiols, we employed CCK-8 assay to test the inhibition rate of PCG. The final concentration was 1 μM and the assay lasted 72 h. PPG was used as a control prodrug. As shown in Figure S17, PCG could not inhibit much less cell growth than PPG.

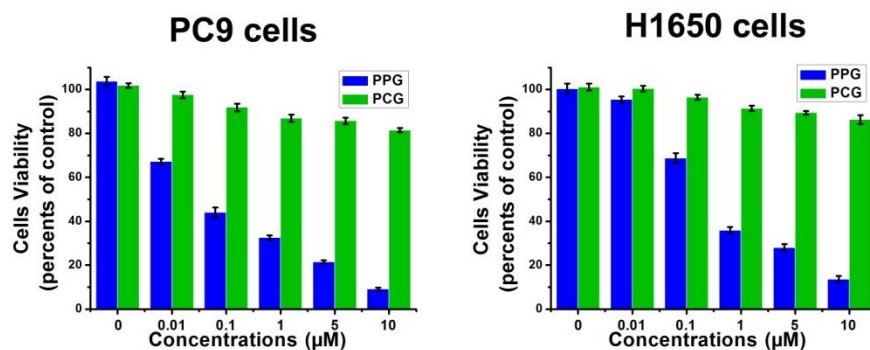


Figure S17. Cell viabilities of PC9 cells and H1650 cells. The cells were treated with PPG and PCG with 0, 0.01, 0.1, 1, 5 and 10 μM for 72 h, then measured using CCK-8 kit ($n = 6$ independent experiments).

21. The prodrug stability and the release of Gefitinib assay in the presence of albumin

We performed the HPLC experiments to investigate the stability of the prodrug (PPG) in the presence of albumin and to determine the albumin binding rate of prodrug. Bovine serum albumin (BSA, 0.04 g/mL) was prepared in HEPES buffer (10 mM, pH 7.4, 0.5% DMSO, 0.4% Tween 80) at 37°C. And PPG (10 μ M) was dissolved in the above solution.

Seven standard samples of PPG in 0.04 g/mL BSA (0.5, 1.0, 2.0, 5.0, 10.0, 15.0 and 20.0 μ M) were prepared to generate the calibration curve for linearity of the method. PPG were separated on reversed-phase high performance liquid chromatography (RP-HPLC) with a ZORBAX SB-C18 column (4.6 \times 150 mm, 5 μ m), acetonitrile/0.15% (v/v) ammonium acetate (adjusted pH 8.0 with ammonium hydroxide) = (85:15, v/v) as mobile phase at a flow rate of 1.0 mL/min, detection wavelength of 310 nm and column temperature of 37°C, injection volume: 20 μ L. The peak of PPG appeared at 2.06 min (Figure S18a).

To evaluate the stability of the PPG, PPG was dissolved in the 0.04 g/mL BSA solution for 48 h. And the samples were added in the ultrafiltration system (cellulose acetate membrane with 25 KDa molecular weight cut-off) at the time points of 0 h, 6 h, 12 h, 18 h, 24 h, 30 h, 36 h, 42 h, and 48 h. Centrifugations were performed at 37°C, for 10 min at 4000 rpm, resulting in filtrate. The filtrate was performed RP-HPLC analysis. As shown in Figure S18b, the concentration of PPG in the filtrate didn't change in 48 h. The result indicated that the prodrug PPG was stable in the presence of albumin.

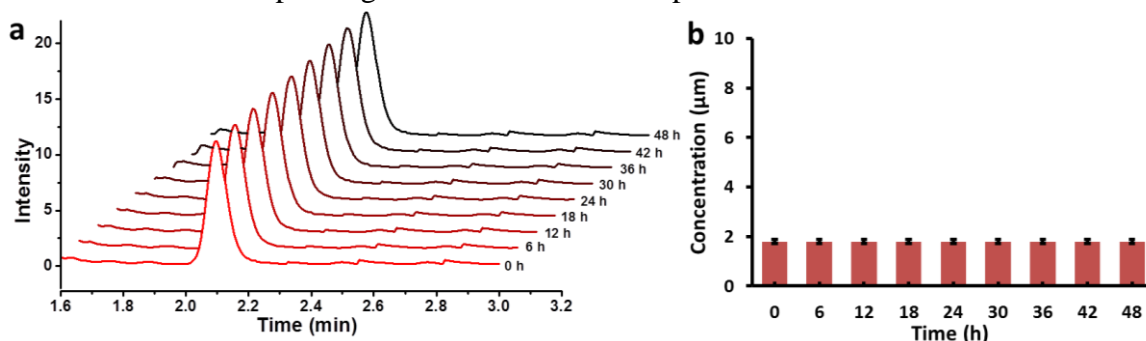


Figure S18. (a) HPLC analysis of PPG in the presence of BSA within 48 h. (b) Quantify the concentration of PPG in the presence of BSA within 48 h.

The fraction of unbound was determined by the following equation [4]:

$$f_u = C_u / C_t$$

Where f_u is the fraction of unbound drug in albumin, C_u is the unbound concentration, and C_t is the total concentration of the analyte in albumin, respectively.

Then the albumin binding rate of prodrug was determined by the ultrafiltration method mentioned above [5]. And the albumin binding rate of prodrug with bovine serum albumin was $78.2 \pm 0.5\%$.

The release of Gefitinib is based on GSH to cleave the disulfide bond. Because the GSH concentration in the plasma was $0.34 \pm 0.11 \mu$ M [6], which was unable to induce the rapid release of Gefitinib. As shown in Figure S18a, none Gefitinib was detected through HPLC. Therefore, nearly no Gefitinib was released in albumin condition.

22. The stability of *Azo*-BODIPY fluorophore

The *Azo*-BODIPY fluorophore had been widely used in bioimaging. The stable experiment was carried out to verify the stability of the dye in the testing solution. As shown in Figure S19, the fluorescent intensity hardly changed under the testing condition within 42 h.

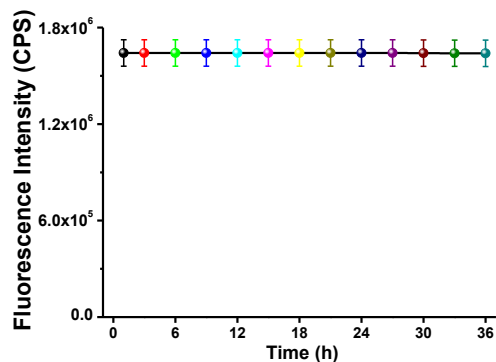


Figure S19. Fluorescent stable of the probe within 42 h. The fluorescence intensity of TPG was acquired every 3 h in the range of 0 - 42 h ($\lambda_{ex/em} = 706/730$ nm). The experiment was accomplished in 10 mM HEPES buffer (pH 7.4, 0.5% DMSO, 0.4% Tween 80) at 37°C. The data were shown as mean (\pm s.d.) ($n = 3$).

23. Another format for Figure 3h and 3i

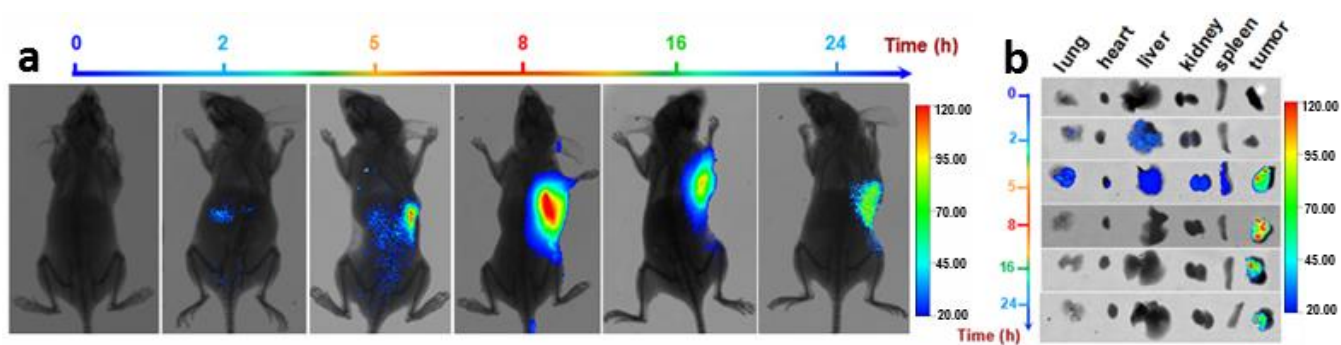


Figure S20. Illustration of Figure 3h and 3i with a lower legend value. (a) Images in Figure 3h with a lower value. (b) Images in Figure 3i with a lower value.

24. References

- [1] (a) Ong, W.; Grindstaff, J.; Sobransingh, D.; Toba, R.; Quintela, J. M.; Peinador, C.; Kaifer, A. E. *J. Am. Chem. Soc.* **2005**, *127*, 3353-3361; (b) Feng, D.; Li, X.; Wang, X.; Jiang, X.; Li, Z. *Tetrahedron* **2004**, *60*, 6137-6144.
- [2] Kumar, R.; Han, J.; Lim, H. J.; Ren, W. X.; Lim, J. Y.; Kim, J. H.; Kim, J. S. *J. Am. Chem. Soc.* **2014**, *136*, 17836-17843.
- [3] Gao, M.; Yu, F.; Chen, H.; Chen, L. *Anal. Chem.* **2015**, *87*, 3631-3638.
- [4] Voelkner NMF, Voelkner A, Costa J, Sy SKB, Hermes J, Weitzel J, Morales S, Derendorf H, Dermal pharmacokinetics of pyrazinamide determined by microdialysis sampling in rats. *Int J Antimicrob Agents.* **2017**; doi: 10.1016/j.ijantimicag.
- [5] Chen Q, He H, Luo S, Xiong L, Li P. A novel GC-MS method for determination of chrysophanol in rat plasma and tissues: Application to the pharmacokinetics, tissue distribution and plasma protein binding studies. *J Chromatogr B Analyt Technol Biomed Life Sci.* **2014**; 973C:76-83.
- [6] Wendel A, Cikryt P. The level and half-life of glutathione in human plasma. *FEBS Lett.* **1980**; 120:209-211.